Reactions of Laser-Ablated Molybdenum and Tungsten Atoms with Dioxygen. Resolved Infrared Spectra of Natural Molybdenum and Tungsten Isotopic Oxides in Argon Matrices

William D. Bare, Philip F. Souter, and Lester Andrews*

Department of Chemistry, University of Virginia, Charlottesville, Virginia 22901

Received: June 15, 1998; In Final Form: August 10, 1998

Laser-ablated molybdenum and tungsten atoms were reacted with dioxygen and ^{18}O-substituted dioxygen. The products of these reactions were isolated in solid argon matrices at 10 K and studied by matrix infrared spectroscopy. Analysis of spectra enabled identification of reaction products, which included MoO_2, (O_2)-MoO_2, MoO_3, WO, WO_2, $(O_2)WO_2$, and WO_3. Resolution of isotopic splitting due to natural isotopic abundance of the metal verified the presence of a single metal atom in these molecules and allowed for calculation of bond angles for the molybdenum and tungsten dioxide molecules and their dioxygen complexes.

Introduction

The bulk oxides of molybdenum and tungsten have been widely investigated in recent years and have been found to have several industrially significant properties. Principle among these are the ability to function as catalysts in many important reactions including cracking and isomerization of alkanes and alkenes,[1−3] the oxidation of organic substrates by hydrogen peroxide,[4] and the photoinduced oxidation of water to dioxygen.[5] These species have also found usefulness in electrochromic devices[6−8] and in pH-sensing electrodes.[9]

On the molecular level, the metal oxides have received comparatively little attention. These species have been investigated spectroscopically by isolating the products formed by passing oxygen over a hot metal surface,[10,11] by matrix isolation of evaporated bulk oxides,[10−12] and by photolysis of saturated carbonyls in oxygen-doped matrices.[13,14] Molybdenum and tungsten oxides have also been produced by hollow cathode sputtering techniques.[15,16] These methods have all produced important results, but a large fraction of polymers are formed because of the high temperatures required for evaporation of the molecules under study,[10,11] and there is disagreement on assignments for many of these molecules.

Direct reaction of dioxygen with laser-ablated metal atoms followed by matrix isolation of products has proven to be a very effective means of forming and studying small metal oxide molecules.[17−20] This method is particularly advantageous for the study of metals with very high melting points, such as those discussed here, because the focused laser heats only the small volume of metal being evaporated. In this paper, we report a matrix-isolation FTIR spectroscopic investigation of the oxides of molybdenum and tungsten formed by reaction of dioxygen with the laser-ablated metal atoms. This work is a continuation of a similar report on the oxides of chromium[19] where chromium dioxide, CrO_2, was formed in high yield and natural chromium isotopic splittings were observed for both stretching fundamentals.

Of particular importance in this work is the use of isotopic substitution for identification of product species and for calculation of bond angles for C_{2v} molecules.[21−25] Frequency shifts of infrared absorptions resulting from isotopic substitution are characteristic not only of the masses of the atoms involved but also of the structure and symmetry of the molecule. For this reason, isotopic substitution (using $^{16}O_2$, $^{16}O^{18}O$, and $^{18}O_2$) is extremely effective in extracting information about the identity and structure of molecules under investigation. Isotopic frequency shifts are particularly important for the study of molybdenum and tungsten, which are isotopically rich metals, with seven and four naturally occurring isotopes of significant abundance, respectively.[26] The combination of intentional substitution with isotopically enriched oxygen and the natural isotopic abundance metals has produced extraordinarily rich spectra. The spectroscopic conditions employed here permitted resolution of these isotopic patterns for most molecules, enabling accurate calculations of bond angles for WO_2, MoO_2, and their dioxygen complexes.

Experimental Section

The technique and apparatus for laser ablation and matrix isolation FTIR spectroscopy have been described previously.[27] Molybdenum (Goodfellow) and tungsten (Johnson-Matthey) targets were mounted on rotating (1 rpm) stainless steel rods. The pulsed (10 Hz, 20−40 mJ/pulse) Nd:YAG laser (1064 nm fundamental) was focused on the target through a hole in the 10 K CsI window. Dilute (0.2−1.0%) oxygen in argon was introduced through the gas nozzle and co-deposited with the ablated metal atoms on the cryogenic window. Combinations of isotopically enriched oxygen ($^{18}O_2$, "mixed" = $^{16}O_2/^{18}O_2$, and "scrambled" = $^{16}O_2/^{16}O^{18}O/^{18}O_2$) samples were used in subsequent experiments. Spectra were recorded on a Nicolet 550 or Nicolet 750 FTIR spectrophotometer using 0.5 or 0.125 cm^{-1} resolution. Matrices were subjected to broadband photolysis by a medium-pressure Hg arc lamp (Philips, 175 W, with globe removed, 240−580 nm) and to several annealing−recooling cycles, with spectra recorded after each event.

Results

Infrared spectra of matrices containing reaction products of dioxygen with molybdenum are shown in Figures 1 and 2, featuring annealing behavior and resolved metal isotopes, respectively. Spectra from reactions with tungsten are shown in Figures 3 and 4. Observed infrared absorptions are listed in Tables 1−3. In discussions below, bands will be generally be referred to by a single frequency, although in the case of vibrations with substantial metal character, several isotopic bands have been resolved and identified. Absorptions given in the text below will refer to the peak maxima in the case of unresolved bands and to the most abundant isotope (^{98}Mo or ^{184}W) in the cases with resolved metal isotopic spectra.

Density functional theory calculations were preformed on expected monoxide, dioxide, and trioxide products using the

10.1021/jp9826266 CCC: $15.00
Published on Web 10/02/1998

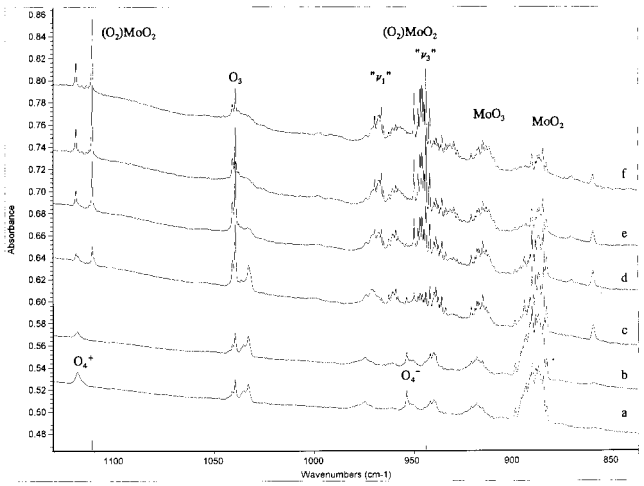

Figure 1. Infrared spectra in the 1130−840 cm^{-1} region for laser-ablated Mo atoms co-deposited with O_2 (0.5%) in excess argon at 10 K using 0.5 cm^{-1} resolution: (a) after co-deposition for 2 h at 10 K; (b) after broadband photolysis; (c) after annealing to 25 K; (d) after annealing to 30 K; (e) after annealing to 35 K; (f) after annealing to 40 K.

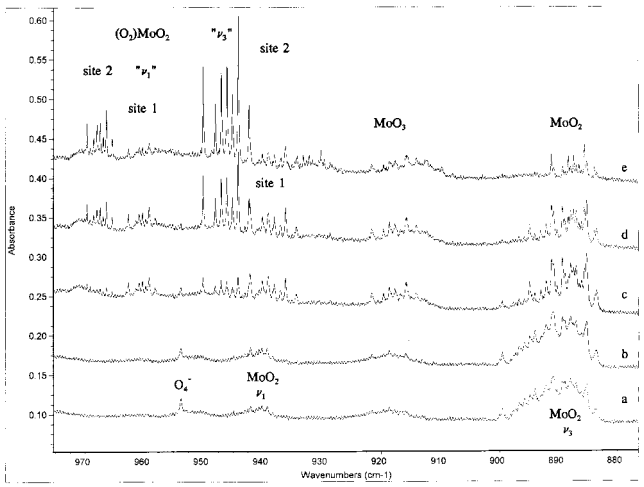

Figure 2. Infrared spectra in the 970−880 cm^{-1} region for laser-ablated Mo atoms co-deposited with O_2 (0.5%) in excess argon at 10 K using 0.125 cm^{-1} resolution: (a) after co-deposition for 2 h at 10 K; (b) after broadband photolysis; (c) after annealing to 25 K; (d) after annealing to 30 K; (e) after annealing to 35 K.

Gaussian 94 program[28] operating on an SP2 computer. Calculations were done using the BP86 functional,[29] with the D95 basis set for oxygen[30] and the LanL2DZ basis set and pseudopotentials for molybdenum and tungsten.[31] Calculated geometries and vibrational frequencies for these molecules are given in Table 4.

Discussion

Molybdenum has seven naturally abundant isotopes (^{92}Mo, 14.8%; ^{94}Mo, 9.3%; ^{95}Mo, 15.9%; ^{96}Mo, 16.7%; ^{97}Mo, 9.5%; ^{98}Mo, 34.1%; ^{100}Mo, 9.7%), and tungsten has four major natural isotopes (^{182}W, 26.4%; ^{183}W, 14.4%; ^{184}W, 30.6%; ^{186}W, 28.4%).[26] These resolved mass distributions are plotted in Figure 5 along with an unresolved mass profile to contrast the appearance of unresolved and resolved metal-isotope-dependent spectra for vibrations of a single metal atom.

The relationship between vibrational frequencies of isotopomers is described by Wilson, Decius, and Cross[32] and by Herzberg.[33] What has generally been underappreciated, however,

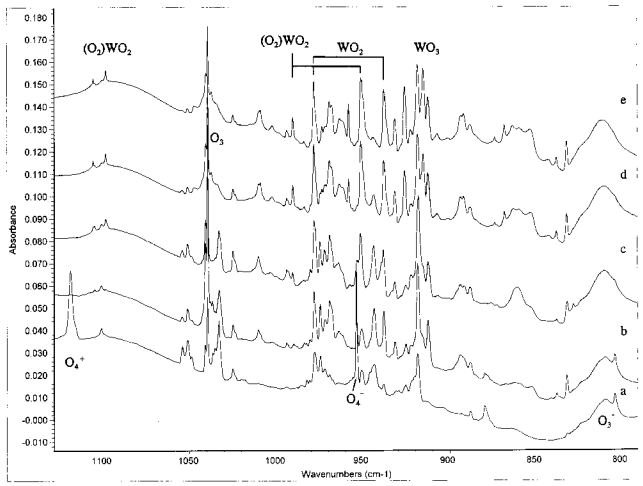

Figure 3. Infrared spectra in the 1130−790 cm^{-1} region for laser-ablated W atoms co-deposited with O_2 (0.5%) in excess argon at 10 K using 0.5 cm^{-1} resolution: (a) after co-deposition for 2 h at 10 K; (b) after broadband photolysis; (c) after annealing to 25 K; (d) after annealing to 30 K; (e) after annealing to 35 K.

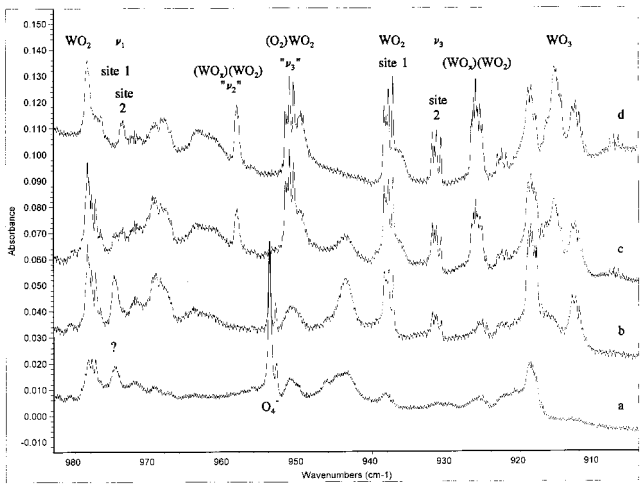

Figure 4. Infrared spectra in the 980−900 cm^{-1} region for laser-ablated W atoms co-deposited with O_2 (0.5%) in excess argon at 10 K using 0.125 cm^{-1} resolution: (a) after co-deposition for 2 h at 10 K; (b) after broadband photolysis; (c) after annealing to 25 K; (d) after annealing to 30 K.

is the significance of isotopic substitution for the determination of molecular valence angles in small molecules. For triatomic C_{2v} molecules, the antisymmetric (ν_3) stretching motion can provide a determination of the valence angle, since ν_3 is alone in its symmetry class, and calculations based on this mode are free from errors introduced by coupling with other modes.

For triatomic C_{2v} molecules with the structure T−A−T (terminal, apical, terminal), the frequency of the antisymmetric (ν_3) stretching mode is proportional to the square root of both the **F**-matrix element, F_{33}, and the **G**-matrix element, G_{33}. The **G**-matrix element for this mode is given by eq 1

$$G_{33} = \frac{1}{m_T} + \frac{1}{m_A}(1 - \cos\alpha) \qquad (1)$$

where m_T and m_A are the masses of the terminal and apex atoms, respectively, and α is the bond angle. It is assumed that the force constant matrix is the same for each isotopomer and is therefore factorable in computing the ratios of isotopic frequencies. The ratio of two isotopic frequencies is the square root

TABLE 1: Infrared Absorptions (cm^{-1}) for Products of Reactions of Molybdenum with Oxygen in Solid Argon

label	$^{16}O_2$	$^{18}O_2$	ratio	assignment
A	1119.3	1056.0	1.0599	$(O_2)MoO_2$ (site 2)
A	1111.2	1.048.8	1.0595	$(O_2)MoO_2$ (site 1)
B	969.7	920.7	1.0532	$(O_2)^{92}MoO_2$ (ν_1) (site 2)
	966.4	917.5	1.0532	$(O_2)^{98}MoO_2$ (ν_1)
C	962.7	914.9	1.05225	$(O_2)^{92}MoO_2$(ν_1) (site 1)
	959.2	911.1	1.05279	$(O_2)^{98}MoO_2$(ν_1)
D	950.1	907.5	1.04694	$(O_2)^{92}MoO_2$ (ν_3) (site 2)
	944.2	901.2	1.04771	$(O_2)^{98}MoO_2$ (ν_3)
E	942.1	893.7	1.05416	$^{92}MoO_2$ (ν_1) (site 1)
	939.3	890.8	1.05445	$^{98}MoO_2$ (ν_1)
F	942.4	900.1	1.04699	$(O_2)^{92}MoO_2$ (ν_3) (site 1)
	936.2	893.8	1.04744	$(O_2)^{98}MoO_2$ (ν_3)
G	921.6	880.5	1.04668	$^{92}MoO_3$
	915.8	874.3	1.04747	$^{98}MoO_3$
H	899.5	858.9	1.04727	$^{92}MoO_2$ (site 3)
	894.0	853.0	1.04807	$^{98}MoO_2$
I	894.9	854.7	1.04703	$^{92}MoO_2$ (site 4)
J	891.9	851.2	1.04782	$^{92}MoO_2$ (ν_3) (site 1)
	885.5	845.3	1.04756	$^{98}MoO_2$ (ν_3)
K	890.7	850.8	1.04696	$^{92}MoO_2$ (ν_3) (site2)
	885.1	845.0	1.04746	$^{98}MoO_2$ (ν_3)
L	860.0	813.6	1.05701	$Mo^+O_3^-$
M	686.0	653.5	1.0497	Mo_xO_y (ref 12)
N	528.6	507.9	1.0396	$(O_2)^{92}MoO_2$ (site 2)
	522.8	502.7	1.0400	$(O_2)^{98}MoO_2$

of the ratio the **G**-matrix elements for the isotopomers.

$$\frac{\nu_A}{\nu_{A'}} = \sqrt{\frac{1/m_T + (1/m_A)(1 - \cos\alpha)}{1/m_T + (1/m_{A'})(1 - \cos\alpha)}} \quad (2)$$

or

$$\frac{\nu_T}{\nu_{T'}} = \sqrt{\frac{1/m_T + (1/m_A)(1 - \cos\alpha)}{1/m_{T'} + (1/m_A)(1 - \cos\alpha)}} \quad (3)$$

If frequencies and isotopic masses are known for any pair of iostopomers (TAT, TA′T or TAT, T′AT′), the ratio of the measured frequencies provides a route to calculation of the bond angle α. Two groups[22,25] have explained that the effects of anharmonicity are such that substitution at the apical position and use of eq 2 yield a calculated bond angle that is too low, while substitution at the terminal positions and use of eq 3 predict a bond angle that is too high. These anharmonicity errors are approximately equal, and therefore, the average of these two numbers is an excellent measurement of the true bond angle, as has been demonstrated for SO_2 and O_3.[22−24] The isotopic frequency data sets generated in this investigation have permitted the calculation of bond angles for the bent MoO_2 and WO_2 molecules and their dioxygen complexes.

Another source of information that may be derived from isotopic substitution is the differentiation between and identification of symmetric and antisymmetric stretching modes of C_{2v} molecules, based on isotopic substitution at the apical position. The symmetric stretching mode (ν_1) has the same symmetry (a_1) as the bending mode and is therefore more susceptible to mode-mixing effects and is less useful for quantitative determinations. However, when these two modes are widely separated (as is the case here), these effects are small and qualitative information can be readily obtained. Isotopic frequency ratios derived from ν_1 modes have the same relationship as those of the ν_3 modes except that the sign in the geometric term of the **G**-matrix element, G_{11}, is reversed.

$$\frac{\nu_A}{\nu_{A'}} = \sqrt{\frac{1/m_T + (1/m_A)(1 + \cos\alpha)}{1/m_T + (1/m_{A'})(1 + \cos\alpha)}} \quad (4)$$

The result of this sign change is that, for molecules with obtuse angles, the effect of isotopic substitution at the apical position is proportionally less for the ν_1 mode than for the corresponding ν_3 mode. As a result, the family of bands produced from isotopic substitution at the apical position has significantly larger spacings between adjacent bands for the ν_3 mode relative to the ν_1 mode. In most cases for molybdenum and tungsten, this difference is significant enough such that there is an easily recognizable qualitative difference in the appearance of bands (i.e., the overall bandwidth) due to the ν_1 and ν_3 modes.

MoO. A previous investigation on the oxides of molybdenum has reported an infrared band at 893.5 cm^{-1} with an ^{18}O counterpart near 850 cm^{-1}, which was assigned to the MoO molecule.[15] Spectra produced in the current study indicate that four sets of bands (H, I, J, and K, discussed below with MoO_2) are present in the 890 cm^{-1} region. However, the resolution of band splitting due to isotopes of molybdenum (which was not possible previously) makes clear that none of these bands has an isotopic (16/18) ratio that is consistent with assignment to MoO.

The isotopic resolution of these four band sets gave a total of 23 resolved bands for the $^{16}O_2$ experiment and 21 resolved bands for the experiment with $^{18}O_2$, allowing for the calculation of 20 isotopic ($\nu(16)/\nu(18)$) frequency ratios. Isotopic pairs of bands due to MoO are expected to exhibit a frequency ratio ($\nu(16)/\nu(18)$) near 1.0508 (1.0500 for ^{92}Mo and 1.0516 for ^{100}Mo). Of the bands in this region, no frequency ratio was greater than 1.048 07. The average ratio was 1.047 37 with a standard deviation of 0.000 36 (less than 0.05%). These ratios are not consistent with assignment to MoO but are appropriate for the MoO_2 molecule to be described below.

It has been found that the combination of changes in mass and relativistic effects for diatomic transition metal compounds (specifically oxides) is such that vibrational frequencies are typically very close for second- and third-row metal species of the same group.[34] One may consider TiO, ZrO, and HfO (987.8, 958.6, and 958.3 cm^{-1}, respectively)[35] and VO, NbO and TaO (983.6, 970.6, and 1014.2 cm^{-1}, respectively[20]). In light of this correlation, it is likely that the WO molecule provides a good estimate of the vibrational frequency of MoO. As will be discussed below, bands due to the WO molecule have been observed near 1051 cm^{-1} in an argon matrix, and it is not likely that the MoO species will deviate significantly from this frequency. Also, this estimation is in agreement with BP86 calculations, which predicted a frequency of 1043.8 cm^{-1} for the MoO molecule. This having been said, no bands were observed in the current investigation in either of these regions (1050 or 890 cm^{-1}), which can be attributed to MoO. If one assumes that the MoO_2/WO_2 relationship will hold for MoO/WO, then the MoO fundamental will be near 1000 cm^{-1}. Until a proper isotopic spectrum of MoO is recorded, the present 1000 $\pm$ 20 cm^{-1} estimate is suggested for MoO and should be used in MoO studies (for example, ref 36) *instead* of the incorrect matrix assignment.[15]

In this regard, Bauschlicher et al. have predicted properties for CrO and MoO using higher levels of theory.[37] Since the SDCI method was the best predictor of harmonic frequency for CrO ($^5\Pi$), the SDCI prediction for the MoO ($^5\Pi$) harmonic frequency is 1035 cm^{-1}.

MoO_2. Four sets of bands (899.5, 894.9, 891.1, and 890.7 cm^{-1}) were observed here following sample deposition. Some

TABLE 2: Resolved Isotopic Absorptions of Molybdenum Oxide Products in Argon

label	16	18	ratio	assignment
B	969.7	920.7	1.053 22	$(O_2)^{92}MoO_2$ "ν_1"
	968.5	919.8	1.052 95	$(O_2)^{94}MoO_2$ (site 2)
	968.0	919.3	1.052 98	$(O_2)^{95}MoO_2$
	967.4	918.7	1.053 70	$(O_2)^{96}MoO_2$
	966.9	918.1	1.053 15	$(O_2)^{97}MoO_2$
	966.4	917.5	1.053 30	$(O_2)^{98}MoO_2$
	965.4	916.4	1.053 47	$(O_2)^{100}MoO_2$
C	962.7	914.9	1.052 25	$(O_2)^{92}MoO_2$ "ν_1"
		913.6		$(O_2)^{94}MoO_2$ (site 1)
	960.8	912.9	1.052 47	$(O_2)^{95}MoO_2$
	960.3	912.3	1.052 61	$(O_2)^{96}MoO_2$
	959.8			$(O_2)^{97}MoO_2$
	959.2	911.1	1.052 79	$(O_2)^{98}MoO_2$
	958.1	909.9	1.052 97	$(O_2)^{100}MoO_2$
D	950.1	907.5	1.046 94	$(O_2)^{92}MoO_2$ "ν_3"
	948.0	905.3	1.047 17	$(O_2)^{94}MoO_2$ (site 2)
	947.0	904.3	1.047 22	$(O_2)^{95}MoO_2$
	946.1	903.2	1.047 50	$(O_2)^{96}MoO_2$
	945.1	902.2	1.047 55	$(O_2)^{97}MoO_2$
	944.2	901.2	1.047 71	$(O_2)^{98}MoO_2$
	942.4	899.3	1.047 93	$(O_2)^{100}MoO_2$
E	942.1	893.7	1.054 16	$^{92}MoO_2$ (ν_1) (site 1)
	941.1	892.7	1.054 22	$^{94}MoO_2$ (ν_1)
	940.6	892.2	1.054 25	$^{95}MoO_2$ (ν_1)
	940.2	891.8	1.054 27	$^{96}MoO_2$ (ν_1)
	939.7	891.3	1.054 30	$^{97}MoO_2$ (ν_1)
	939.3	890.8	1.054 45	$^{98}MoO_2$ (ν_1)
	938.3	889.9	1.054 39	$^{100}MoO_2$ (ν_1)
F	942.4	900.1	1.046 99	$(O_2)^{92}MoO_2$ "ν_3"
	940.1	897.8	1.047 12	$(O_2)^{94}MoO_2$ (site 1)
	939.1	896.9	1.047 05	$(O_2)^{95}MoO_2$
	938.1	895.9	1.047 10	$(O_2)^{96}MoO_2$
	937.1	894.6	1.047 51	$(O_2)^{97}MoO_2$
	936.2	893.8	1.047 44	$(O_2)^{98}MoO_2$
	934.3	891.7	1.047 77	$(O_2)^{100}MoO_2$
G	921.6	880.5	1.046 68	$^{92}MoO_3$ (e)
	919.6	878.3	1.047 02	$^{94}MoO_3$ (e)
	918.6	877.3	1.047 08	$^{95}MoO_3$ (e)
	917.7	876.3	1.047 24	$^{96}MoO_3$ (e)
	916.8	875.3	1.047 41	$^{97}MoO_3$ (e)
	915.8	874.3	1.047 47	$^{98}MoO_3$ (e)
	914.0	872.2	1.047 92	$^{100}MoO_3$ (e)
H	899.5	858.9	1.047 27	$^{92}MoO_2$ (ν_3) (site 3)
		856.8		$^{94}MoO_2$ (ν_3)
	896.7	855.9	1.047 67	$^{95}MoO_2$ (ν_3)
	895.8	854.9	1.047 84	$^{96}MoO_2$ (ν_3)
	894.9			$^{97}MoO_2$ (ν_3)
	894.0	853.0	1.048 07	$^{98}MoO_2$ (ν_3)
	892.1			$^{100}MoO_2$ (ν_3)
I	894.9	854.7	1.047 03	$^{92}MoO_2$ (ν_3) (site 4)
J	891.1	851.2	1.046 88	$^{92}MoO_2$ (ν_3) (site 1)
	889.2	849.2	1.047 10	$^{94}MoO_2$ (ν_3)
	888.2	848.2	1.047 16	$^{95}MoO_2$ (ν_3)
	887.3	847.2	1.047 33	$^{96}MoO_2$ (ν_3)
	886.4	846.2	1.047 51	$^{97}MoO_2$ (ν_3)
	885.5	845.3	1.047 56	$^{98}MoO_2$ (ν_3)
	883.8	843.5	1.047 78	$^{100}MoO_2$ (ν_3)
K	890.7	850.8	1.046 90	$^{92}MoO_2$ (ν_3) (site 2)
	888.8	848.8	1.047 13	$^{94}MoO_2$ (ν_3)
	887.9	847.8	1.047 30	$^{95}MoO_2$ (ν_3)
	886.9	846.8	1.047 35	$^{96}MoO_2$ (ν_3)
	886.0	845.9	1.047 41	$^{97}MoO_2$ (ν_3)
	885.1	844.9	1.047 58	$^{98}MoO_2$ (ν_3)
	883.4	843.1	1.047 80	$^{100}MoO_2$ (ν_3)
N	528.0	507.9	1.039 57	$(O_2)^{92}MoO_2$ "ν_3"
	526.5	506.4	1.039 69	$(O_2)^{94}MoO_2$ (site 2)
	525.6	505.3	1.040 17	$(O_2)^{95}MoO_2$
	524.4	502.7	1.039 59	$(O_2)^{96}MoO_2$
	523.6	501.4	1.039 09	$(O_2)^{97}MoO_2$
	522.6			$(O_2)^{98}MoO_2$
	521.0			$(O_2)^{100}MoO_2$

band overlap prevented complete isotopic resolution of all bands; however, bands were resolved for each set, and all seven isotopic bands were clearly resolved for the 891.1 and 890.7 cm^{-1} sets, J and K, as given in Table 2. These bands all decreased on sequential annealing, although the first two sites decreased more at lower temperatures than the last two sites. Above 30 K, the 890.7 cm^{-1} set also decreased and the bands in the 891.1 cm^{-1} set became the most prominent, as seen in Figure 2. The clear isotopic pattern of the seven bands is evidence of a single molybdenum atom in the absorbing species. In the experiment with isotopically scrambled O_2, a 1:2:1 triplet was observed, indicating the presence of two equivalent oxygen atoms. The

TABLE 3: Resolved Tungsten Isotopic and Other Absorptions (cm^{-1}) for Oxide Products in Solid Argon

$^{16}O_2$	$^{18}O_2$	ratio	assignment
1105.5	1043.2	1.0597	$(O_2)WO_2$ (site 1)
1098.1	1036.3	1.0597	$(O_2)WO_2$ (site 2)
1054.9	999.7	1.05522	^{182}WO
	999.5		^{183}WO
1054.5	999.3	1.05524	^{184}WO
1054.0	998.8	1.05527	^{186}WO
1051.6			^{182}WO
1051.3			^{183}WO
1051.1	996.2	1.05501	^{184}WO
1050.7			^{186}WO
993.9	940.2	1.05734	$(O_2)^{182}WO_2$ (ν_1) (site 1)
	940.1		$(O_2)^{183}WO_2$ (ν_1)
	940.0		$(O_2)^{184}WO_2$ (ν_1)
	939.8		$(O_2)^{186}WO_2$ (ν_1)
990.3	937.1	1.0568	$(O_2)OWO$ (ν_1) (site 2)
978.3	925.9	1.05694	$^{182}WO_2$ ν_1 (site 1)
	925.7		$^{183}WO_2$
	925.6		$^{184}WO_2$
	925.3		$^{186}WO_2$
978.4	928.4	1.05386	$X-O^{182}WO$
978.2	928.2	1.06387	$X-O^{183}WO$
977.9	927.9	1.05389	$X-O^{184}WO$
977.4	927.3	1.05403	$X-O^{186}WO$
973.8	923.2	1.05459	$^{182}WO_2$ ν_1 (site 2)
973.6	922.8		$^{184}WO_2$
973.3			$^{186}WO_2$
969.6	920.2	1.05368	ν_3?
969.4	919.9	1.05381	
969.1	919.7	1.05371	
968.5	919.1	1.05375	
958.4	906.7	1.05702	$(WO_x)(OWO)$ ν_1
	906.6	1.05715	$(WO_x)(OWO)$ ν_1
958.2	906.4	1.05716	$(WO_x)(OWO)$ ν_1
958.0	906.2		$(WO_x)(OWO)$ ν_1
951.7	903.8		$(O_2)^{182}WO_2$
951.5	903.6		$(O_2)^{183}WO_2$
951.2	903.2		$(O_2)^{184}WO_2$
950.6	902.6		$(O_2)^{156}WO_2$
938.3	891.4	1.05261	$^{182}WO_2$ ν_3 (site 1)
938.0	891.1	1.05263	$^{183}WO_2$ ν_3 (site 1)
937.7	890.8	1.05265	$^{184}WO_2$ ν_3 (site 1)
937.1	890.2	1.05268	$^{186}WO_2$ ν_3 (site 1)
931.9	885.2	1.05276	$^{182}WO_2$ ν_3 (site 2)
931.6	884.9	1.05277	$^{183}WO_2$ ν_3 (site 2)
931.3	884.6	1.05279	$^{184}WO_2$ ν_3 (site 2)
930.7	884.0	1.05283	$^{186}WO_2$ ν_3 (site 2)
926.6	880.4	1.05248	$(WO_x)(OWO)$
926.3	880.1	1.05249	$(WO_x)(OWO)$ ν_3
926.0	879.8	1.05251	$(WO_x)(OWO)$
925.7	879.5	1.05253	$(WO_x)(OWO)$
925.4	879.2	1.05255	$(WO_x)(OWO)$
925.1	878.9	1.05257	$(WO_x)(OWO)$
923.0	876.9	1.05257	$^{182}WO_3$ (e) (site 2)
922.7	876.6	1.05259	$^{183}WO_3$
922.5	876.3	1.05272	$^{184}WO_3$
921.9	875.7	1.05276	$^{186}WO_3$
918.7	871.6	1.05358	$^{182}WO_3$ (e) (site 1)
918.5			$^{183}WO_3$
918.3			$^{184}WO_3$
917.8			$^{186}WO_3$
832.0	787.5	1.0565	W_2O_2
498.0	475.5	1.0473	$(O_2)WO_2$
560.7	532.0	1.0539	?

TABLE 4: Density Functional Theory (BP86/D95/LanL2DZ) Calculations for Mo and W Oxides

molecule	electronic state	M−O bond length, Å	O−M−O bond angle, deg	frequency, cm^{-1} (intensity, km/mol)
MoO	triplet	1.664		1043.8 (139)
MoO_2	triplet	1.723	113.5	299.5 (0.2) a_1
				923.6 (188) b_2
				964.3 (52) a_1
MoO_3	singlet	1.734	108.6	277.4 (25) a_1
				329.7 (1 × 2) e
				929.9 (155 × 2) e
				960.6 (3) a_1
WO	triplet	1.714		978.4 (106)
WO_2	triplet	1.720	112.2	314.4 (1) a_1
				933.1 (142) b_2
				993.5 (40) a_1
WO_3	singlet	1.735	106.2	297.2 (12) a_1
				340.2 (1 × 2) e
				919.1 (118 × 2) e
				988.9 (1) a_1

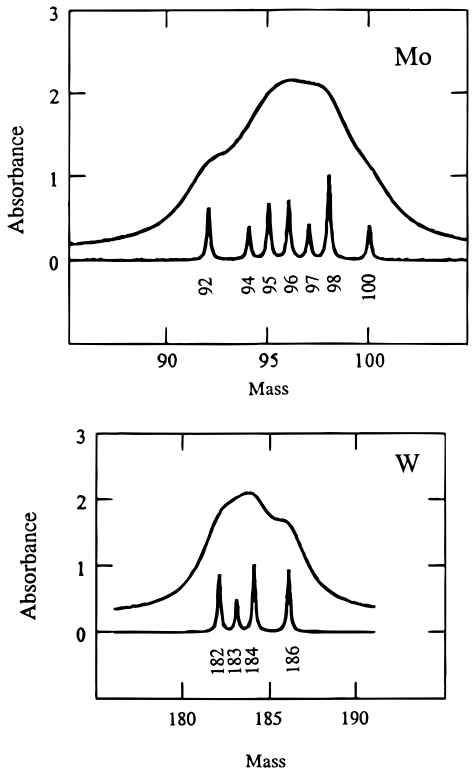

Figure 5. Mass distributions of natural Mo and W isotopes plotted for unresolved and resolved infrared spectra.

new intermediate band was observed at 856.9 cm^{-1}. As mentioned above, the observed isotopic (16/18) ratios for these bands are consistent with the MoO_2 molecule, which was predicted by BP86 calculations to have a strong antisymmetric vibration at 923.6 cm^{-1}.

The width of the band groups ($^{92}Mo-^{100}Mo$) was 7.3 cm^{-1} for both J and K. The ^{100}Mo bands were not observed for the first two sets H and I, but the splitting between the observed bands was approximately 0.9 cm^{-1}/mass unit, indicating a similar group width. This indicates that each set of bands is due to an antisymmetric (ν_3, b_1) stretching vibration and is assigned accordingly to one of four matrix sites of the ν_3 vibration of MoO_2.

A weaker set of bands near 942 cm^{-1} (E) was observed following deposition of the matrix and showed the same annealing behavior as the family of bands near 890 cm^{-1}. This set of bands has a group width of approximately 3.8 cm^{-1}, indicating that it is a symmetric (ν_1, a_1) stretching vibration, and is assigned here as the ν_1 vibration of MoO_2. A visual comparison (see Figure 2) of the band sets at 942 and 890 cm^{-1} provides an excellent example of the clear, qualitative difference in the appearance of band sets that differentiates ν_1 and ν_3 modes.

Sixteen $^{16}O^{n}Mo^{16}O/^{18}O^{n}Mo^{18}O$ pairs were identified, allowing 16 calculations of the bond angle upper limit for the MoO_2 molecule. The calculations yielded an upper limit of 125 ± 1°. Similarly, more than 40 $O^{n}MoO/O^{n'}MoO$ pairs were used to calculate the bond angle lower limit, yielding a result of 119 ± 3°. A determination of 122 ± 4° is proposed for the O−Mo−O bond angle. This is in excellent agreement with the analogous calculations for O−Cr−O, which gave 132 ± 2° upper and 125 ± 2° lower limits and a 128 ± 4° average angle.[19] This experimentally determined bond angle is higher but in accord with the BP86 calculated prediction of 113.5° for MoO_2.

MoO_3. Infrared bands at 976 and 922 cm^{-1} and 920−910 cm^{-1} have previously been assigned to the MoO_3 molecule.[11,12] Spectra produced in these investigations have replicated a set of bands at 915.8 cm^{-1} but did not find evidence for a set of tracking bands at 976 cm^{-1}. Furthermore, BP86 calculations have indicated that the symmetric (a_1) stretch for this molecule has extremely low intensity and likely will not be observed. Accordingly, we suggest that the 976 cm^{-1} band reported previously is dominated by higher oxides.

When $^{18}O_2$ is substituted, the band at 915.8 cm^{-1} is shifted to 874.3 cm^{-1}. The scrambled O_2 experiment yielded weak bands corresponding to the pure $^{16}O_2$ and pure $^{18}O_2$ bands but did not produce any new, mixed isotopic bands of measurable intensity. This isotopic splitting behavior is consistent with the 2:1:1:2 splitting pattern that is expected for the degenerate Mo−O stretching mode of the MoO_3 molecule, if the intermediate bands are too weak to be observed.[38] Considering the complex nature of mixed isotopic spectra and the substantial isotopic dilution involved, this seems quite reasonable. A tempting assignment to MoO is again ruled out on the basis of isotopic frequency ratios, which are much too low to be due to MoO. One should also note that this assignment is in excellent agreement with the BP86 calculation, which predicted an intense degenerate stretching mode at 929.9 cm^{-1} for the MoO_3 molecule.

$(O_2)MoO_2$. Several sets of bands (B−D and F) grew in after annealing cycles. Band sets at C and F appeared at 25 K, grew at 30 K, and gradually decreased at higher temperatures. Those at B and D were initially weaker but continued to grow through at least 40 K, becoming the strongest bands in that spectral region. The behavior of these bands tracks with the set of bands labeled A at 1119.3 and 1111.2 cm^{-1}. The annealing behavior exhibited by these bands is characteristic of bands due to complexes, which often form as a result of ligands diffusing in the matrix. The 1.0597 ± 0.0002 frequency ratio for the A band is consistent with the expected shift for the O−O stretch of ligated O_2.

The bands at B−D and F all have isotopic shifts consistent with assignment to Mo−O stretching modes in $(O_2)MoO_2$ complexes. The frequency shifts of the symmetric and antisymmetric MoO stretches for this complex are expected to be very close to those of isolated MoO_2 if the O_2 ligands are not strongly bound or if their vibrations do not couple with those of the MoO_2 fragment. This appears to be the case in this instance. The group widths ($^{92}Mo-^{100}Mo$) of the B and C band groups (4.3 and 4.6 cm^{-1}, respectively) indicate that these are

symmetric (ν_1) stretching modes, while those of the D and F bands (7.7 and 8.1 cm^{-1}, respectively) are due to antisymmetric stretching motions. It is also important that the bands due to ν_3 modes are considerably more intense than those of the ν_1 modes.

The frequency ratios of the antisymmetric O−Mo−O stretch can be used to calculate a bond angle in the same manner as that described for the isolated molecule (again, assuming weak coupling). The resolved D and F band sets provide 14 TAT/T′AT′ isotopic pairs and 41 TAT/TA′T isotopic pairs for determination of upper and lower limits to the bond angle of the MoO_2 fragment. These data yield a calculated upper limit of 124 ± 2° and a lower limit of 119 ± 4°, suggesting an O−Mo−O bond angle of 121 ± 4°, which is essentially unchanged for MoO_2 on complexation by dioxygen.

In the lower spectral region, a band at 522.8 cm^{-1} (N) also grew in on annealing and tracked with the A−D and F bands. Substitution with $^{18}O_2$ shifted this band to 502.7 cm^{-1}, giving an isotopic frequency ratio of 1.039 98, which is in good agreement with that expected for the antisymmetric vibration of

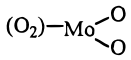

The above molecule may be *approximately* modeled as a molybdenum atom between O_2 and two O atoms. By use of this model, isotopic frequency ratios are expected to have increased dependence on the mass of the central metal atom and decreased dependence on the mass of the O_2 units. This trend is observed for this band, which has a small $\nu(16)/\nu(18)$ ratio (1.040 vs 1.047 for MoO_2) and a large $\nu(92)/\nu(100)$ ratio (1.013 vs 1.008 for MoO_2).

This dioxygen complex with MoO_2 is expected to have the C_{2v} structure observed and calculated for the analogous O_2 complex with NbO_2.[20]

Other Absorptions. The 860.0 cm^{-1} absorption appears on annealing and shifts to 813.6 cm^{-1} with $^{18}O_2$ (1.0570 ratio), which is characteristic of an O−O stretching mode. The band profile certainly indicates that Mo is not involved in the vibration. This band is most likely due to an ozonide species $Mo^+O_3^-$, which is expected in this region,[39] although the yield was too low to observe mixed isotopic components.

WO. Two resolved bands at 1054.5 and 1051.1 cm^{-1} were observed following deposition. The upper band decreased following annealing as the lower band became the dominant site. When $^{18}O_2$ was used, these bands shifted to 999.3 and 996.2 cm^{-1}. For the upper band, all four tungsten isotopic bands were identified (see Table 3) in both the $^{16}O_2$ and $^{18}O_2$ experiments. For the lower band, only one of the $^{18}O_2$ bands was resolved. These bands allowed five calculations of $^n W^{16}O/^n W^{18}O$ isotopic frequency ratios (1.055 20, 1.052 25, 1.055 22, 1.055 23, and 1.055 11), which are all in excellent agreement with the expected harmonic ratios for WO. Assignment of these bands to WO is also in accord with the somewhat lower 978.4 cm^{-1} frequency prediction from BP86 calculations.

The argon matrix bands observed here are in excellent agreement (0.2 cm^{-1} difference for the major site) with the sputtering matrix work of Green and Ervin[16] and the gas-phase WO ground-state fundamental value of 1053.7 cm^{-1}.[40,41] The argon matrix sites cause blue and red shifts of the WO fundamental by only 0.7 and 2.6 cm^{-1}, respectively, from the gas-phase values.

WO_2. Infrared absorptions for WO_2 isolated in krypton have previously been reported by Green and Ervin[16] at 937.2 and 975.5 cm^{-1}. These assignments are in excellent agreement with BP86 calculations reported here, which have predicted frequencies of 930.0 and 960.6 cm^{-1} for the antisymmetric and symmetric stretching modes of WO_2. The current work has produced isotopically resolved bands in argon at 937.7 and 978.3 cm^{-1}. On initial inspection, it appears that the upper of these bands (ν_1) is of comparable intensity to the lower (ν_3) band, which is contrary to the expected 3:1 intensity ratio predicted by calculations and observed previously.[16] However, the spectral features near 978 cm^{-1} indicate that another band may be present in this area, giving increased absorbance to the 978.3 cm^{-1} band. Also, the band group width ($\nu(182)-\nu(186)$) of the ν_3 mode is much larger than that of the ν_1 mode, and as a result, the integrated area under these peaks is much closer to the expected 3:1 ratio than are the simple peak heights. Substitution with $^{18}O_2$ shifted these bands to 890.8 and 925.6 cm^{-1}. Intermediate isotopic components (16,18) for these bands were observed at 902.2 and 962.8 cm^{-1}, but tungsten isotopic peaks were not resolved.

A second set of bands with similar isotopic shifts was observed approximately 5−10 cm^{-1} to the red of these bands at 931.3 and 973.6 cm^{-1}. Isotopic substitution with $^{18}O_2$ shifted the lower of these bands to 884.6 cm^{-1}; the ^{18}O counterpart of the upper band was too weak to be conclusively identified. The red-shifted bands are assigned as sites of the WO_2 stretching modes.

All four natural tungsten isotopic bands were resolved for both the pure ^{16}O and pure ^{18}O bands of the WO_2 antisymmetric stretch. This provided four pairs of terminally substituted isotopomers and 12 apically substituted isotopomer pairs. Bond angle calculations based on these data gave an upper limit of 127 ± 1° and a lower limit of 122 ± 2°. A bond angle of 124 ± 4° is therefore determined here for WO_2, which is slightly higher than the 114 ± 3° value deduced by Green and Ervin from the unresolved tungsten isotopic band profile but near the 122 ± 4° and 128 ± 4° values for MoO_2 and CrO_2.

WO_3. BP86 calculations for the WO_3 species have predicted an intense degenerate stretching mode at 919.2 cm^{-1}, supporting the earlier assignment by Green and Ervin of a 918.3 cm^{-1} absorption in argon to WO_3. Experiments reported here produced a band at 918 cm^{-1}, which is also consistent with this assignment. Substitution with $^{18}O_2$ shifted this band to 872 cm^{-1}, and mixed and scrambled experiments produced weak intermediate components at 892.4 and 881.0 cm^{-1} in accord with the pattern expected for the degenerate stretching mode of a trigonal pyramidal species. Annealing increases the 918 cm^{-1} absorption and satellites at 915 and 913 cm^{-1}, which are probably due to perturbed WO_3. This is in agreement with the $W(CO)_6$ photolysis work, which assigned a 914 cm^{-1} band to WO_3. Isotopic resolution of the WO_3 bands was not achieved in the current study.

$(O_2)WO_2$. Bands were observed at 951.2 and 990.3 cm^{-1}, which increased as a result of annealing. These bands are each approximately 12 cm^{-1} to the blue of the bands assigned to the stretching modes of the WO_2 molecule and are assigned as the analogous stretching motions of the complexed species (O_2)-WO_2. The formation of complexes that are slightly blue-shifted relative to the isolated molecule was observed for the MoO_2 species discussed above. A pair of site bands at 1105.5 and 1098.1 cm^{-1} also appear following annealing and track with the bands at 951.2 and 990 cm^{-1}. These bands shifted to 1043.2 and 1036.3 cm^{-1} with $^{18}O_2$. The 1.0597 isotopic frequency ratio of these bands is consistent with assignment to the ligated O_2 stretching mode of the $(O_2)WO_2$ complex.

The isotopic resolution of the antisymmetric stretch of the WO_2 fragment in the $(O_2)WO_2$ complex allows a calculation of the O−W−O bond angle. Four $^{16}O^nW^{16}O/^{18}O^nW^{18}O$ pairs and 12 $O^nWO/O^{n'}WO$ pairs were used to determine upper and lower limits bond angle limits of 123 ± 1° and 114 ± 4°. A bond angle of 119 ± 5° is therefore determined for the O_2 complex, which is essentially unchanged for WO_2 on complexation by O_2.

In the lower spectral region, a new annealing band appeared at 498.0 cm^{-1} and shifted to 475.5 cm^{-1} in the $^{18}O_2$ experiment. This low (1.047 32) $\nu(16)/\nu(18)$ isotopic ratio is characteristic of the antisymmetric vibration of the tungsten atom between O_2 and the two O atoms in $(O_2)WO_2$, as described previously for $(O_2)MoO_2$. This complex of dioxygen and WO_2 is expected to have the C_{2v} structure calculated and observed for the analogous complex of O_2 and TaO_2.[20]

W_2O_2. The 832.0 cm^{-1} band in the region expected for bridged W−O stretching vibrations and the shift to 787.5 cm^{-1} gives a $\nu(16)/\nu(18)$ ratio just above that for WO. The mixed $^{16}O_2/^{18}O_2$ study gave a 1:2:1 triplet, with bands at 832.0, 808.5, and 787.5 cm^{-1}. This suggests a tentative assignment to a cyclic W_2O_2 species formed by dimerization of WO molecules.

Other Absorptions. There are other absorptions, presumably those of W_xO_y, in these experiments that cannot be identified, which include the 978, 942, and 879 cm^{-1} peaks. The most interesting of these, the 978 cm^{-1} band present on deposition, shows resolved W isotopes and 16/18 ratios slightly larger than ν_3 of WO_2 and grows slightly on annealing.

Charged Species. Charged oxygen species are observed in these and earlier metal experiments involving O_2 with yields depending on laser power.[17−20] These include O_4^+ (1118 cm^{-1}), O_4^- (953.8 cm^{-1}), and O_3^- (804 cm^{-1}).[42−44] The O_4^- and O_3^- species are formed by capture of electrons from laser ablation during the condensation process. The O_4^+ cation probably arises from photoionization of O_2 with hard radiation in the laser plume followed by union with another O_2 molecule during condensation. All three of these charged oxygen species are photosensitive, and they have high infrared oscillator strengths. Although it is reasonable to expect MoO_2^- and WO_2^- to be observed, no evidence was found for these molecular anions.

Reaction Mechanisms. Gas-phase studies[45−48] have found that both ground ($^7S_3$) and excited-state Mo and W atoms react with O_2 with nearly gas kinetic rates and no pressure dependence, which suggests that the O−O bond is easily activated. These studies followed the metal atoms and not the products formed; however, MoO and WO have been observed in gas phase.[36,49] The growth of MoO_2 and WO_2 on matrix photolysis and the absence of growth on matrix annealing suggest some activation energy for insertion reaction 5:

$$M + O_2 \rightarrow (MO_2)^* \xrightarrow{\text{decompose}} MO + O \qquad (5a)$$

$$\xrightarrow{\text{argon relax}} MO_2 \qquad (5b)$$

In the present laser ablation−matrix isolation experiments, metal atom reactions with O_2 occur *during condensation* with excess argon, where many gas collisions with argon atoms rapidly relax the initial $(MO_2)^*$ insertion product and favor relaxation reaction 5b relative to decomposition reaction 5a. In the gas phase, we expect the decomposition reaction to dominate. The lack of MoO observation here, in view of its optical spectroscopic observation in the gas phase,[36] is probably due to our lower sensitivity of detection.

Conclusions

The reaction of laser-ablated tungsten and molybdenum atoms with dioxygen has produced several metal oxide products, including MoO_2, MoO_3, $(O_2)MoO_2$, WO, WO_2, WO_3, and $(O_2)WO_2$. These products were analyzed by matrix infrared spectroscopy and were identified by isotopic shifts and correlation with BP86 calculations. These results corroborate many assignments of previous investigators but challenge previous assignments to MoO and to the symmetric stretch of MoO_3.

Of principle importance in this work is the use of resolved isotopic metal and oxygen infrared spectra to determine bond angles for C_{2v} molecules and their O_2 complexes. Accurate measurement of isotopic frequencies due to the antisymmetric stretching motions provides a route to the calculation of bond angles for MoO_2, $(O_2)MoO_2$, WO_2, and $(O_2)WO_2$. For each of these molecules and complexes, a large number of consistent calculations were performed, and bond angles were determined to within 4°.

Acknowledgment. We gratefully acknowledge support for this research from NSF Grant CHE 97-00116.

References and Notes

(1) Sellem, S.; Potvin, C.; Manoli, J. M.; Maquet, J.; Djegamariadassou, G. *Catal. Lett.* **1996**, *41*, 89.
(2) Matsuda, T.; Sakagami, H.; Takahashi, N. *J. Chem. Soc., Faraday Trans.* **1997**, *93*, 2225.
(3) Meijers, S.; Gielgens, L. H.; Ponec, V. *J. Catal.* **1995**, *156*, 147.
(4) Conte, V.; Difuria, F.; Moro, S. *J. Phys. Org. Chem.* **1996**, *9*, 329.
(5) Erbs, W.; Desilvestro, J.; Borgarello, E.; Grätzel, M. *J. Phys. Chem.* **1984**, *88*, 4001.
(6) Bechinger, C.; Oefinger, G.; Herminghaus, S. *J. Appl. Phys.* **1993**, *74*, 4527.
(7) Ho, K. C.; Rukavina, T. G.; Greenberg, C. B. *J. Electrochem. Soc.* **1994**, *141*, 2061.
(8) Batchelor, R. A.; Burdis, M. S.; Siddle, J. R. *J. Electrochem. Soc.* **1996**, *143*, 1050.
(9) Kriksunov, L. B.; Macdonald, D. D.; Millett, P. J. *J. Electrochem. Soc.* **1994**, *141*, 94.
(10) Weltner, W., Jr.; McLeod, D., Jr. *J. Mol. Spectrosc.* **1965**, *17*, 277.
(11) Hewett, W. D., Jr.; Newton, J. H.; Weltner, W., Jr. *J. Phys. Chem.* **1975**, *79*, 2640.
(12) Serebrenikov, L. V.; Maltsev, A. A. *Vestn. Mosk. Univ. Ser. 2: Khim.* **1976**, *1*, 38.
(13) Almond, M. J.; Crayston, J. A.; Downs, A. J.; Poliakoff, M.; Turner, J. J. *Inorg. Chem.* **1986**, *25*, 19.
(14) Almond, M. J.; Downs, A. J. *J. Chem. Soc., Dalton Trans.* **1988**, 809.
(15) Bates, J. K.; Gruen, D. M. *J. Mol. Spectrosc.* **1979**, *78*, 284.
(16) Green, D. W.; Ervin, K. M. *J. Mol. Spectrosc.* **1981**, *89*, 145.
(17) Chertihin, G. V.; Saffel, W.; Yustein, J. T.; Andrews, L.; Neurock, M.; Ricca, A.; Bauschlicher, C. W., Jr. *J. Phys. Chem.* **1996**, *100*, 5261−5273.
(18) Chertihin, G. V.; Bare, W. D.; Andrews, L. *J. Phys. Chem. A* **1997**, *101*, 5090.
(19) Chertihin, G. V.; Bare, W. D.; Andrews, L. *J. Chem. Phys.* **1997**, *107*, 2798.
(20) Zhou, M. F.; Andrews, L. *J. Phys. Chem. A*, in press.
(21) White, D.; Seshardi, K. S.; Dever, D. F.; Mann, D. E.; Linevski, M. J. *J. Chem. Phys.* **1963**, *39*, 2463.
(22) Allavena, M.; Rysnik, R.; White, D.; Calder, V.; Mann, D. E. *J. Chem. Phys.* **1969**, *50*, 3399.
(23) Andrews, L.; Spiker, R. C., Jr. *J. Phys. Chem.* **1972**, *76*, 3208.
(24) Green, D. W.; Reedy, G. T. *J. Chem. Phys.* **1978**, *69*, 544.
(25) Green, D. W.; Ervin, K. M. *J. Mol. Spectrosc.* **1981**, *88*, 51.
(26) *CRC Handbook*; Chemical Rubber Publishing Co.: Boca Raton, FL, 1985.
(27) Hassanzadeh, P.; Andrews, L. *J. Phys. Chem.* **1992**, *96*, 9177.
(28) Frisch, M. J.; Trucks, G. W.; Schlegel, H. B.; Gill, P. M. W.; Johnson, B. G.; Robb, M. A.; Cheeseman, J. R.; Keith, T.; Petersson, G. A.; Montgomery, J. A.; Raghavachari, K.; Al-Laham, M. A.; Zakrzewski, V. G.; Ortiz, J. V.; Foresman, J. B.; Cioslowski, J.; Stefanov, B. B.; Nanayakkara, A.; Challacombe, M.; Peng, C. Y.; Ayala, P. Y.; Chen, W.; Wong, M. W.; Andres, J. L.; Replogle, E. S.; Gomperts, R.; Martin, R. L.; Fox, D. J.; Binkley, J. S.; Defrees, D. J.; Baker, J.; Stewart, J. P.; Head-

Gordon, M.; Gonzalez, C.; Pople, J. A. *Gaussian 94, Revision B.1*.; Gaussian, Inc.: Pittsburgh, PA, 1995.

(29) Perdew, J. P. *Phys. Rev. B* **1986**, *33*, 8822. Becke, A. D. *J. Chem. Phys*. **1993**, *98*, 5648.

(30) Dunning, T. H., Jr.; Hay, P. J. In *Modern Theoretical Chemistry*; Schaefer, H. F., III, Ed.; Plenum: New York, 1976.

(31) Hay, P. J.; Wadt, W. R. *J. Chem. Phys.* **1985**, *82*, 299.

(32) Wilson, E. B., Jr.; Decius, J. C.; Cross, P. C. Molecular Vibratons; McGraw-Hill: New York, 1955.

(33) Herzberg, G. *Molecular Spectra and Molecular Structure. II. Infrared and Raman Spectra of Polyatomic Molecules*; Van Nostrand: Princeton, NJ, 1945.

(34) Pyykko, P. *Chem. Rev.* **1988**, *88*, 563.

(35) Chertihin, G. V.; Andrews, L. *J. Phys. Chem.* **1995**, *99*, 6356.

(36) Hamrick, Y. M.; Taylor, S.; Morse, M. D. *J. Mol. Spectrosc.* **1991**, *146*, 274.

(37) Darling, J. H.; Ogden, J. S. *J. Chem. Soc., Dalton Trans.* **1972**, 2496.

(38) Bauschlicher, C. W., Jr.; Nelin, C. J.; Bagus, P. S. *J. Chem. Phys.* **1985**, *82*, 3265.

(39) Spiker, R. C., Jr.; Andrews, L. *J. Chem. Phys.* **1973**, *59*, 1851.

(40) Gatterer, A.; Krishnamurty, S. G. *Nature (London)* **1952**, *169*, *543.*

(41) Huber, K. P.; Herzberg, G. *Constants of Diatomic Molecules*; Van Nostrand: New York, 1979.

(42) Thompson, W. E.; Jacox, M. E. *J. Chem. Phys.* **1989**, *91*, 3826.

(43) Hacaloglu, J.; Andrews, L. Unpublished results.

(44) Chertihin, G. V.; Andrews, L. *J. Chem. Phys.* **1998**, *108*, 6404.

(45) Lian, L.; Mitchell, S. A.; Rayner, D. M. *J. Phys. Chem.* **1994**, *98*, 11637.

(46) Campbell, M. L.; McLean, R. E.; Harter, J. S. S. *Chem. Phys. Lett.* **1995**, *235*, 497.

(47) Wakabayashi, T.; Ishikawa, Y.; Arai, S. *Chem. Phys. Lett.* **1996**, *256*, 543.

(48) Campbell, M. L.; McLean, R. E. *J. Chem. Soc., Faraday Trans.* **1995**, *91*, 3787.

(49) Samoilova, A. N.; Efremov, Y. M.; Gurvich, L. V. *J. Mol. Spectrosc.* **1981**, *86*, 1.